JOC The Journal of Organic Chemistry

Article

pubs.acs.org/joc

Electrochemically Induced Ring-Opening/Friedel–Crafts Arylation of Chalcone Epoxides Catalyzed by a Triarylimidazole Redox Mediator

Nan-ning Lu,[†] Ni-tao Zhang,[†] Cheng-Chu Zeng,*[,†] Li-Ming Hu,[†] Seung Joon Yoo,[‡] and R. Daniel Little*[,‡]

[†]College of Life Science & Bioengineering, Beijing University of Technology, Beijing 100124, China

[‡]Department of Chemistry & Biochemistry, University of California, Santa Barbara, California 93106-9510, United States

Supporting Information

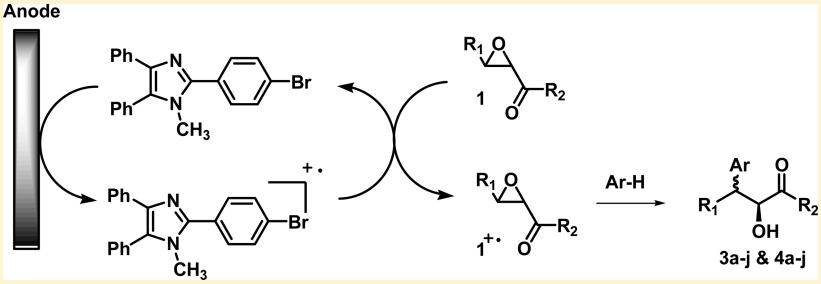

ABSTRACT: The indirect anodic oxidation of chalcone epoxides in the presence of electron-rich heteroarenes mediated by a triarylimidazole (Med) was investigated by cyclic voltammetry (CV) and controlled potential electrolysis. The CV results indicate that a homogeneous electron transfer between $Med^{\bullet+}$ and chalcone epoxides is facilitated by an electron-rich heteroarene that serves as an arylation reagent. The preparative scale electrolysis generated epoxide-ring-opened/Friedel–Crafts arylation products in moderate to good yields. The fact that only a catalytic amount of charge was required suggests that $Med^{\bullet+}$ initiates a chain reaction. In addition, overoxidation of the products is avoided even though their oxidation potential is less than that of the starting chalcone epoxides.

1. INTRODUCTION

Organic electrosynthesis constitutes a powerful, versatile, and environmentally friendly protocol.[1] The direct electron transfer between the working electrode and a substrate generates a cation radical in an oxidation or an anion radical in a reduction.[2] Occasionally, the direct electron transfer can lead to unwanted side reactions, and the in situ generated reactive species may polymerize on the electrode surface leading to passivation. In these instances, it is advantageous to employ a redox mediator and perform an indirect electrolysis.[3] In an indirect oxidation, the redox catalyst initially undergoes a heterogeneous oxidation at the working electrode. The resulting cation radical then engages in a homogeneous electron transfer to oxidize the substrate and simultaneously regenerate the redox catalyst. An indirect electrolysis is generally performed at a potential that is less than that required for the direct process; consequently, the input energy is reduced and greater functional group selectivity/compatibility can be achieved.[3] In this context, the development and selection of an appropriate redox catalyst is critical to ensuring the success of an indirect electrolysis.

We have recently developed a novel class of organic redox catalysts based upon the triarylimidazole (TAI) scaffold.[4−7] These redox catalysts (30 examples) are easy to synthesize, and their oxidation potential can be adjusted to encompass a wide range (>700 mV, from 0.77 to 1.44 V vs Ag/AgCl) by simple modification of the substituents appended to the aromatic rings.[4] In an effort to increase the stability of the cation radical and enhance the influence of the substituents on the peak potential, a fused TAI corresponding to the [9,10-*d*]-phenanthroimidazole framework, was synthesized.[5] In addition, the electron transfer kinetics of the TAI mediator, 2-(4-bromophenyl)-1-methyl-4,5-diphenyl-1*H*-imidazole (BMDPI), has been investigated and compared with the popular organic redox catalyst, tris(4-bromophenyl)amine.[6] In practice, BMDPI has proven to be effective for the functionalization of benzylic C–H bonds leading to an aldehyde, ketone, or benzoate as shown in Scheme 1.[7]

The present investigation was initiated with an eye toward expanding the scope of transformations to which the TAI mediators might be applied. We chose the electrochemical oxidation of chalcone epoxides (structure, see Figure 1), mediated by BMDPI.[8] The processes were conducted in the presence of a variety of electron-rich arenes that were intended to serve as arylating reagents. We are pleased to report that the chemistry, described below in detail, occurred using only a substoichiometric amount of charge, features high chemical selectivity, and avoids overoxidation of the product. This

Received: September 26, 2014
Published: December 2, 2014

   dx.doi.org/10.1021/jo5022184 | *J. Org. Chem.* 2015, 80, 781–789

Scheme 1. Indirect Anodic Oxidation of Benzylic Alcohols and Ethers Mediated by 2-(4-Bromophenyl)-1-methyl-4,5-diphenyl-1*H*-imidazole (BMDPI)

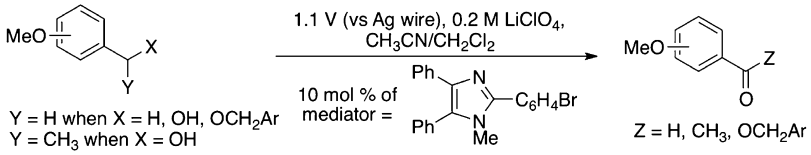

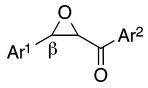

Figure 1. Structure of chalcone epoxides.

present studies further demonstrate that TAIs are versatile redox catalysts in promoting chemical transformations.

2. RESULTS AND DISCUSSION

Before conducting a preparative-scale electrolysis, the chalcone epoxides were examined using cyclic voltammetry. One to three oxidation peak(s) and no cathodic peak were observed in the potential range of 0.0−2.0 V vs $Ag/AgNO_3$ (0.1 M in CH_3CN). The first oxidation peak for a series of chalcone epoxides **1** is listed in Table 1. Note that the potential is dependent upon the electronic character of the substituents appended to the β-aryl group, Ar^1 (Figure 1), while independent of those appended to Ar^2. For example, E_{OX}^1 for chalcone epoxides **1a−e**, each bearing two methoxy groups on Ar^1, is the same (1.06 V) even though Ar^2 varies from phenyl (**1a**) to *p*-methoxyphenyl (**1b**), *p*- and *m*-chlorophenyl (**1c** and **1d**), and furan (**1e**). When three methoxy groups are appended to Ar^1 (structure **1f**), E_{OX}^1 decreases to 1.03 V vs $Ag/AgNO_3$. Conversely, the potential shifts positively viz., to 1.36 V vs $Ag/AgNO_3$ (for **1h** and **1i**) when only one methoxy group is appended to Ar^1. When both

Table 1. First Peak Potentials of Chalcone Epoxides and Related Nucleophiles

Substrate	E_{OX}^1 (V)	Substrate	E_{OX}^1 (V)
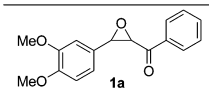 **1a**	1.06	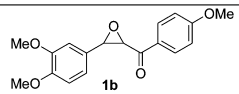 **1b**	1.06
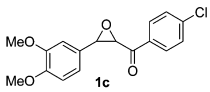 **1c**	1.06	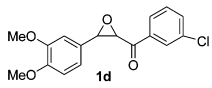 **1d**	1.06
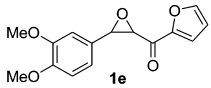 **1e**	1.06	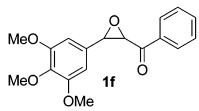 **1f**	1.03
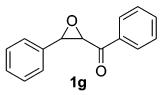 **1g**	>2.00	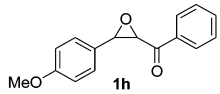 **1h**	1.36
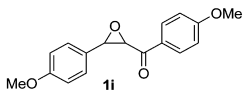 **1i**	1.36	 **2a**	1.52
 **2b**	1.01	 **2c**	1.05
 **2d**	1.36	 **2e**	1.18
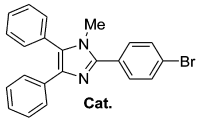 **Cat.**	0.88		

Conditions: 1 mM of substrate in 0.1 M of $LiClO_4/CH_3CN$. Scan rate: 100 mV/s, a GC working electrode, a Pt wire counter electrode, and an $Ag/AgNO_3$ (0.1 M in CH_3CN) reference electrode.

dx.doi.org/10.1021/jo5022184 | J. Org. Chem. 2015, 80, 781−789

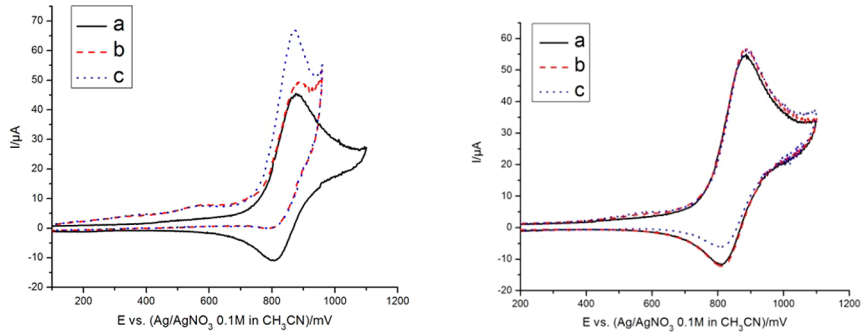

Figure 2. Cyclic voltammogram of BMDPI in the absence and presence of chalcone epoxide **1a** (left), **1g** (right), and furan **2a** at a glassy carbon working electrode, a platinum wire counter, and an Ag/AgCl reference electrode, in 0.1 M of $LiClO_4/CH_3CN$. Scan rate: 100 mV/s. curve a: 1 mmol/L BMDPI; curve b: 1 mmol/L BMDPI, 20 mmol/L **1a** (left) or **1g** (right); c: 1 mmol/L BMDPI, 20 mmol/L **1a** (left) or **1g** (right), with 50 mmol/L of furan.

Ar^1 and Ar^2 correspond to phenyl (structure **1g**), the system is more difficult to oxidize and $E_{OX}{}^1$ increases to more than 2.0 V vs $Ag/AgNO_3$. The oxidation potentials for the arylating reagents, furan (**2a**), pyrroles (**2b** and **2c**), and indoles (**2d** and **2e**) were also measured, and the results are listed in Table 1.

In the present studies, BMDPI was used as a redox catalyst; therefore, its electrochemical behavior was also examined. As reported in our previous publications,[4,6,7] BMDPI exhibits three oxidation peaks and one cathodic peak. The slightly smaller peak current that is observed during the reduction scan of the first redox couple (Figure 2, curve a; E_{OX} 0.88 V and E_{RED} 0.81 V) demonstrates that it is quasi-reversible and that the cation radical of BMDPI is stable on the CV time scale. Thus, it is capable of serving as a redox mediator using a potential corresponding to that of the first oxidation peak.

Next, the electrochemical behavior of BMDPI in the presence of the electron-rich chalcone epoxide **1a** was investigated. As shown in curve b of Figure 2 (left), a slight enhancement of the anodic peak current (45.2 vs 49.4 μA) was observed, accompanied by the disappearance of the cathodic peak, when 20 equiv of chalcone epoxide **1a** was added to the solution of BMDPI in CH_3CN. This observation indicates the occurrence of an endergonic homogeneous electron transfer between $BMDPI^{\bullet+}$ and the epoxide. It is noteworthy that the magnitude of the anodic current for BMDPI increased from 49.4 to 66.9 μA when 20 equiv of furan was added to the mixture of BMDPI and chalcone epoxide **1a**. Since the oxidation potential of furan (1.52 V) is higher than that of the mediator and chalcone epoxide **1a** (1.06 V), the increase in the anodic current at 0.88 V undoubtedly corresponds to a catalytic current and reflects turnover of the mediator.[7] These results demonstrate the efficacy of the electron transfer between $BMDPI^{\bullet+}$ and chalcone epoxide **1a** in the presence of furan.

The voltammetric behavior of BMDPI in the presence of the diphenyl chalcone epoxide **1g** was also examined (Figure 2, right). While nearly identical CV curves were recorded before and after the addition of 20 equiv of **1g** to a solution of BMDPI in CH_3CN, no catalytic current was detected in the presence of furan (curve c, Figure 2, right), although a slight decrease of the cathodic current was observed. This outcome indicates that the electron transfer between chalcone epoxide **1g** and $BMDPI^{\bullet+}$ does not occur even in the presence of furan as a promoter. That BMDPI does not serve as an efficient redox catalyst for the anodic oxidation of chalcone epoxide **1g** is reasonable when one notes that the difference in the oxidation potentials of BMDPI and **1g** is >1.08 V, thereby leading to an insurmountable thermodynamic impasse.

With the CV results as a guide, we selected the reaction of **1a** with **2a** as a model reaction to carry out a controlled potential preparative scale electrolysis at a potential corresponding to the first anodic peak of BMDPI (0.88 V), while recording the change of current as a function of time. As shown in Figure 3,

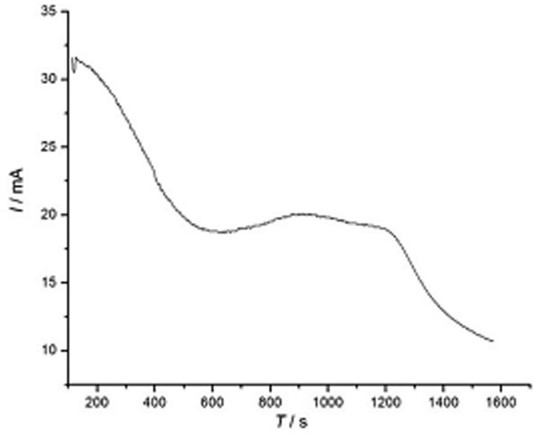

Figure 3. Current−time curve for the anodic oxidation of chalcone epoxide **1a** in the presence of furan mediated by BMDPI.

the initial current amplitude was 31 mA and decreased slowly as the amount of charge increased. The decrease lasted for about 10 min before increasing slightly and then dropping sharply to about 10 mA.[9] At this point, the amount of charge passed was only ~0.5 F/mol, even though TLC analysis showed that the starting **1a** was consumed and two new spots appeared. Considering that only substoichiometric amounts of charge passed before the reaction reached completion (~0.5 F/mol), we suggest that an electrogenerated BMDPI cation radical initiates a chain reaction of the substrate and then re-enters the catalytic cycle. After a conventional workup and column chromatography, two compounds were obtained in a combined yield of 72%, as determined by ^1H NMR using 1,3,5-trimethoxybenzene as an internal standard. All characterization data (NMR, IR, and HRMS) point to the formation of a 1:1.4 mixture of diastereoisomers **3a** and **4a**, derived from ring-opening of chalcone epoxide **1a** followed by a Friedel−Crafts arylation reaction with furan serving as the nucleophile (Table 2, entry 1).

dx.doi.org/10.1021/jo5022184 | J. Org. Chem. 2015, 80, 781−789

Table 2. Ring-Opening/Friedel–Crafts Arylation Reaction of Chalcone Epoxides Mediated by BMDPI

Entry	epoxide	H-Nu	product	Yield (%)[a]
1	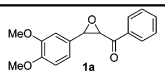 1a	 2a	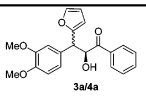 3a/4a	72 (**3a**:**4a** = 1:1.4)
2	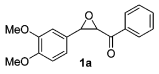 1a	 2a	**3a/4a**	0[b]
3	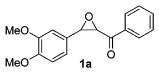 1a	 2b	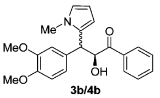 3b/4b	76 (**3b**:**4b** = 1:1.8)
4	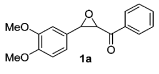 1a	 2c	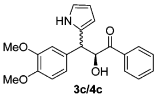 3c/4c	39 (**3c**:**4c** = 1:1.4)
5	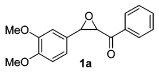 1a	 2d	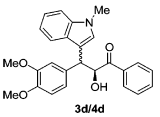 3d/4d	83 (**3d**:**4d** = 1:0.6)
6	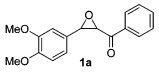 1a	 2e	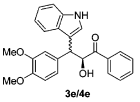 3e/4e	82 (**3e**:**4e** = 1:1)
7	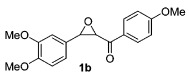 1b	 2a	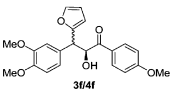 3f/4f	32 (**3f**:**4f** = 1:1)
8	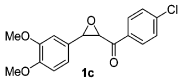 1c	 2a	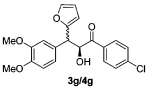 3g/4g	67 (**3g**:**4g** = 1:1.4)
9	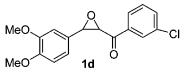 1d	 2a	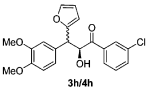 3h/4h	73 (**3h**:**4h** = 1:1.8)
10	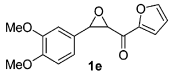 1e	 2a	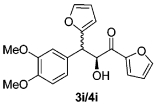 3i/4i	62 (**3i**:**4i** = 1:1.6)
11	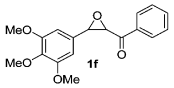 1f	 2a	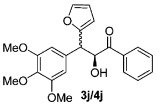 3j/4j	60 (**3j**:**4j** = 1:1.3)
12	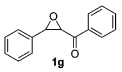 1g	 2a	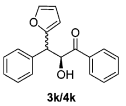 3k/4k	0
13	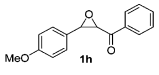 1h	 2a	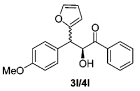 3l/4l	0
14	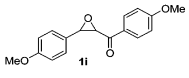 1i	 2a	3m/4m	0

[a]^{1}H NMR yield using 1,3,5-trimethoxybenzene as an internal standard. [b]In the absence of BMDPI.

dx.doi.org/10.1021/jo5022184 | J. Org. Chem. 2015, 80, 781–789

To confirm the importance of BMDPI in the ring-opening and Friedel–Crafts reaction of chalcone epoxide **1a**, a control experiment was performed under identical conditions, but in the absence of BMDPI. Only background levels of current were observed and no reaction took place. Moreover, when the electrolysis was repeated at 1.06 V, the oxidation peak potential of **1a**, the starting material, **1a**, was not consumed and was recovered even after the passage of 2 F/mol of charge (entry 2). These results confirm that the presence of BMDPI is crucial for the ring-opening/Friedel–Crafts arylation reaction.

To explore the scope and generality of the BMDPI-mediated ring-opening/Friedel–Crafts arylation, a variety of arylating reagents were subjected to the reaction conditions in the presence of chalcone epoxide, **1a** (Scheme 2, Table 2, entries 3–6). As shown in Table 2, under the same conditions, *N*-methylpyrrole, **2b**, smoothly afforded adducts **3b**/**4b** in 76% total yield and in a 1:1.8 ratio (entry 3). Pyrrole, **2c**, also worked and gave a 39% yield of **3c**/**4c** in 1:1.4 ratio (entry 4). We attribute the lower yield of **3c**/**4c** to competitive polymerization of pyrrole since it and the starting chalcone epoxide oxidize at nearly the same potentials (1.01 vs 1.06 V). Indole derivatives also proved to be suitable arylation reagents. For example, the BMDPI-induced electrochemical oxidation of chalcone epoxide **1a** in the presence of *N*-methylindole (**2d**) and indole (**2e**) provided good yields of the corresponding adducts **3d**/**4d** and **3e**/**4e** (entries 5 and 6).

To further explore the scope of the chemistry, other chalcone epoxides were investigated with furan serving as the nucleophile, and the results are summarized in Table 2. Chalcone epoxide **1b**, where a methoxy group is located at the *para*-position of the phenmethanone subunit, gave a 32% yield of **3f**/**4f** in a 1:1 ratio (entry 7). However, in the cases of the chloro-substituted analogues **1c** and **1d**, the corresponding adducts, **3g**/**4g** and **3h**/**4h**, were produced in 67% and 73% total yield, respectively (entries 8 and 9). The reaction also tolerates heteroaromatic chalcone epoxides. For example, use of the furyl ketone **1e** led to **3i**/**4i** in 62% yield in a 1:1.6 ratio, under identical conditions. Finally, the BMDPI-induced ring-opening/Friedel–Crafts arylation reaction of chalcone epoxide **1f** and furan proceeded smoothly to afford a 60% combined yield of **3j**/**4j** in a 1:1.3 ratio.

Scheme 2. Electrochemical Oxidative Ring-Opening/Friedel–Crafts Arylation Reaction of Chalcone Epoxides Mediated by BMDPI

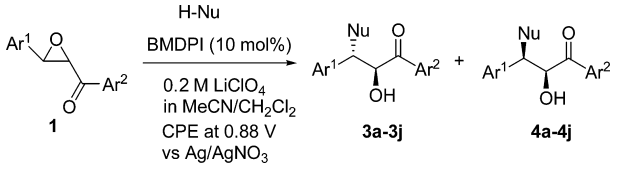

It is noteworthy that in the cases of **1g**, **1h**, and **1i** the reaction did not work under the standard conditions. This outcome is not unexpected, however, since the large potential gap between BMDPI and these epoxides (more than 1.0 V in the case of chalcone epoxide **1g**) renders the homogeneous electron transfer between the chalcone epoxide and BMDPI$^{\bullet+}$ prohibitive. The results are also consistent with the CV experiments described above, where no catalytic current was detected in the presence of **1g** before and after the addition of furan.

Products **3** and **4** are diastereoisomers that differ in stereochemistry at C-3. Spectral characterization was not straightforward as their MS spectra are the same, and the NMR spectra are very similar. Fortunately, we observed that the chemical shift of H^2 in all structures **3** resides downfield of the signal for the same proton in structures **4**. Meanwhile, the reverse is true for H^3 (note Table 3). That is, H^3 is consistently downfield in structure **4**, relative to **3**. Fortunately, the trend is analogous to that observed for diastereomers **3k** and **4k**, whose stereochemistry was confirmed by X-ray crystallographic analysis.[8]

Mechanistically, the triarylaminium-induced Friedel–Crafts alkylation of chalcone epoxides and heteroarenes has been reported to follow a single-electron-transfer initiated chain-reaction pathway.[8] Based on our previous reports[4,6] as well as the CV and preparative-scale results described herein, we propose a similar reaction pathway (Scheme 3). It starts with the anodic oxidation of BMDPI to form BMDPI$^{\bullet+}$, which then engages in a thermodynamically weakly favorable homogeneous electron transfer to oxidize chalcone epoxide **1** to **1**$^{\bullet+}$. Ring opening of the epoxide cation radical leads to the distonic

Table 3. ^{1}H NMR Chemical Shifts for H^2 and H^3 of Structures 3 and 4

	3 (2S, 3R)		4 (2S, 3S)			3 (2S, 3R)		4 (2S, 3S)	
	H^2	H^3	H^2	H^3		H^2	H^3	H^2	H^3
3a, 4a	5.84	3.76	5.53	3.87	**3b, 4b**	5.79	3.83	5.49	3.87
3c, 4c	5.78	3.68	5.48	3.77	**3d, 4d**	5.79	3.66	5.48	3.70
3e, 4e	5.48	3.54	5.28	3.60	**3f, 4f**	5.82	3.66	5.55	3.77
3g, 4g	5.73	3.98	5.65	3.95	**3h, 4h**	5.82	3.46	5.56	3.75
3i, 4i	5.85	3.78	5.80	3.90	**3j, 4j**	5.83	3.82	5.75	3.88
3k, 4k	5.82	3.68	5.50	3.84					

dx.doi.org/10.1021/jo5022184 | J. Org. Chem. 2015, 80, 781–789

Scheme 3. Plausible Mechanism for the BMDPI-Induced Ring-Opening/Friedel–Crafts Arylation of Chalcone Epoxide

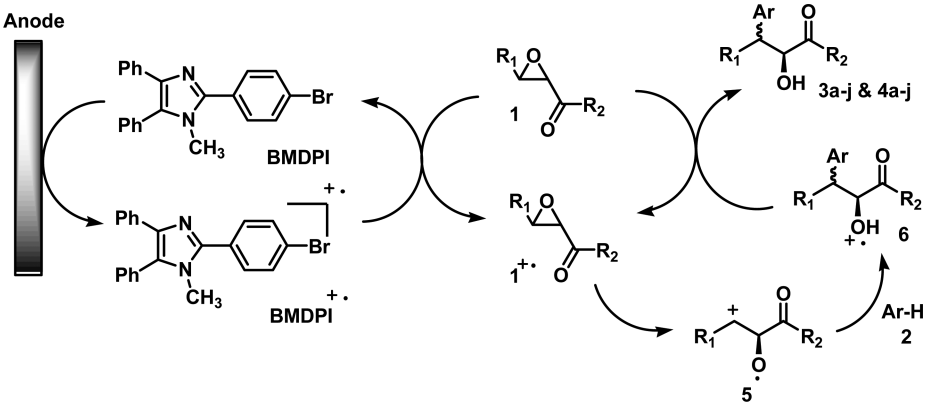

radical cation **5** and sets the stage for nucleophilic capture. In the presence of an electron-rich heteroarene nucleophile **2**, a rapid arylation reaction occurs to afford cation radical **6**. From here, a second homogeneous electron transfer between **6** and the starting epoxide **1** leads to products **3** and **4** and regenerates $\mathbf{1}^{\bullet+}$, thereby allowing it to re-enter the catalytic cycle. Assuming that cation radical **6** is a more powerful oxidizing agent than BMDPI $^{\bullet+}$, an electron transfer between the starting epoxide and **6** will occur in preference to oxidation by BMDPI $^{\bullet+}$. In this manner, only a catalytic amount of charge is required, as observed.

It is significant to note that since the products **3** and **4** are easier to oxidize than the starting materials **1** (0.98 for **3a**, 0.98 V for **4a**, note Table 1 for the chalcone epoxides), the products would suffer from overoxidation if a direct electrolysis were to be performed.[10] Thus, by carrying out a controlled potential electrolysis at the potential of the mediator, overoxidation was avoided. This highlights once again, one of the advantages of carrying out mediated redox processes.[3a]

3. CONCLUSIONS

In summary, the electrochemically mediated ring-opening/Friedel–Crafts arylation of chalcone epoxides with heteroarene nucleophiles has been investigated by cyclic voltammetry and controlled potential electrolysis. The CV of the mediator, BMDPI, in the presence of chalcone epoxide **1a** displayed little change compared with free BMDPI. In contrast, a sizable catalytic current is observed when furan, an arylation reagent, was added. Thus, a furan can facilitate the homogeneous electron transfer between BMDPI and chalcone epoxides. The preparative scale electrolysis of a mixture of chalcone epoxide and an arylation reagent in the presence of BMDPI afforded good yields of ring-opened/Friedel–Crafts arylation products. Since only a catalytic amount of charge was required, an electrogenerated BMDPI cation radical is proposed to initiate a chain reaction. The results further demonstrate the versatility of triarylimidazole redox mediators in indirect electrolysis. Their application to other types of reactions is underway in our laboratory.

4. EXPERIMENTAL SECTION

4.1. Instruments and Reagents. All melting points were measured with an electrothermal melting point apparatus and are uncorrected. IR spectra were recorded using KBr pellets. NMR spectra were recorded with a 400 MHz spectrometer (400 MHz ^{1}H frequency, 100 MHz ^{13}C frequency). Chemical shifts are given as δ values (internal standard: TMS). Coupling constants are reported in hertz. HRMS (ESI) spectra were recorded using Q-TOF as an analyzer. Other chemicals and solvents were obtained from commercial resources and used without further purification.

4.2. Cyclic Voltammetry. Cyclic voltammograms were measured using a Princeton Applied Research 273A potentiostat/galvanostat equipped with electrochemical analysis software, using a conventional three-electrode cell. The working electrode was a glassy carbon disk electrode (ca. ϕ = 3 mm). The auxiliary and reference electrodes in these studies consisted of a Pt wire and an $Ag/AgNO_3$ (0.1 M in CH_3CN), respectively. Glassy carbon was polished with a polishing cloth before each measurement. All electrodes for CV experiments were from CH Instruments, Inc. USA. The concentration of all tested compounds was 1 mmol L^{-1}, while that of the supporting electrolyte was 0.1 mol L^{-1}.

4.3. General Procedure for the Synthesis of Chalcone Epoxides, 1. To a 100 mL round-bottomed flask, maintained in an ice–water bath, was added the chalcone (20 mmol) dissolved in 30 mL of methanol. A mixture of sodium hydroxide (0.8 g, 20 mmol) and 5 mL (40 mmol) of hydrogen peroxide was added slowly to the flask. The resulting mixture was stirred overnight at room temperature. The reaction was monitored by TLC. To quench the reaction, hydrochloric acid (2 M) was added until the pH was less than 7. Then the mixture was poured into 100 mL of water. After cooling, the solid was removed by filtration and recrystallized from ethanol to obtain the pure sample.

*[3-(3,4-Dimethoxyphenyl)oxiran-2-yl]phenylmethanone (**1a**).*[11] Yield: 5.12 g, 90%. Mp: 86–87 °C. ^{1}H NMR ($CDCl_3$, 400 MHz): δ 3.92 (s, 6H), 4.05 (d, J = 1.6 Hz, 1H), 4.30 (d, J = 2.0 Hz, 1H), 6.85 (d, J = 2.0 Hz, 1H), 6.90 (d, J = 8.4 Hz, 1H), 6.98 (dd, J = 8.4, 2.0 Hz, 1H), 7.51 (t, J = 7.6 Hz, 2H), 7.48 (t, J = 7.6 Hz, 1H), 8.03 (d, J = 7.2 Hz, 2H).

*[3-(3,4-Dimethoxyphenyl)oxiran-2-yl]-(4-methoxyphenyl)-methanone (**1b**).*[12] Yield: 5.60 g, 89%. Mp: 77–78 °C. ^{1}H NMR ($CDCl_3$, 400 MHz): δ3.88 (s, 3H), 3.90 (s, 3H), 3.91 (s, 3H), 4.04 (d, J = 2.0 Hz, 1H), 4.26 (d, J = 1.6 Hz, 1H), 6.84 (d, J = 2.0 Hz, 1H), 6.89 (d, J = 8.4 Hz, 1H), 6.95–6.97 (m, 3H), 8.02 (dd, J = 7.2, 2.0 Hz, 2H).

*[3-(3,4-Dimethoxyphenyl)oxiran-2-yl]-4-chlorophenylmethanone (**1c**).* White crystal. Yield: 5.87 g, 92%. Mp: 106–107 °C. ^{1}H NMR ($CDCl_3$, 400 MHz): δ 3.91 (s, 6H), 4.03 (d, J = 1.6 Hz, 1H), 4.23 (d, J = 1.6 Hz, 1H), 6.83 (d, J = 2.0 Hz, 1H), 6.88 (d, J = 8.4 Hz, 1H), 6.96 (dd, J = 8.4, 2.0 Hz, 1H), 7.47 (dd, J = 7.2, 1.6 Hz, 2H), 7.97 (dd, J = 7.2, 1.6 Hz, 2H). ^{13}C NMR (100 MHz, $CDCl_3$): δ 55.9, 56.0, 59.6, 61.1, 108.0, 111.2, 118.9, 127.6, 129.2, 129.8, 133.7, 140.5, 149.4, 149.8, 192.1. HRMS (ESI): calcd for $C_{17}H_{14}ClO_4$ [M − H]: 317.0581, found 317.0581.

*[3-(3,4-Dimethoxyphenyl)oxiran-2-yl]-3-chlorophenylmethanone (**1d**).* Pale yellow crystal. Yield: 5.42 g, 85%. Mp: 129–130 °C. ^{1}H NMR ($CDCl_3$, 400 MHz): δ 3.91 (s, 6H), 4.04 (d, J = 1.6 Hz, 1H), 4.23 (d, J = 1.6 Hz, 1H), 6.83 (d, J = 2.0 Hz, 1H), 6.89 (d, J = 8.4 Hz, 1H), 6.97 (dd, J = 8.0, 2.0 Hz, 1H), 7.44 (t, J = 8.0 Hz, 1H), 7.59–7.61 (m, 1H), 7.90 (d, J = 8.0 Hz, 1H), 8.00 (t, J = 2.0 Hz, 1H). ^{13}C NMR (100 MHz, $CDCl_3$): δ 55.9, 56.0, 59.7, 61.1, 108.0, 111.2, 118.9, 126.5,

dx.doi.org/10.1021/jo5022184 | J. Org. Chem. 2015, 80, 781–789

127.5, 128.3, 130.2, 133.9, 135.2, 136.9, 149.4, 149.8, 192.1. HRMS (ESI): calcd for $C_{17}H_{14}ClO_4$ [M − H] 317.0581, found 317.0579.

*[3-(3,4-Dimethoxyphenyl)oxiran-2-yl]-furan-2-yl-methanone (**1e**).* White crystal. Yield: 4.94 g, 90%. Mp: 125−126 °C. ^{1}H NMR ($CDCl_3$, 400 MHz): δ 3.90 (s, 6H), 4.11 (d, J = 1.6 Hz, 1H), 4.13 (d, J = 2.0 Hz, 1H), 6.61 (dd, J = 3.6, 1.6 Hz, 1H), 6.81 (d, J = 2.0 Hz, 1H), 6.87 (d, J = 8.4 Hz, 1H), 6.95 (dd, J = 8.4, 2.0 Hz, 1H), 7.47 (d, J = 3.6 Hz, 1H), 7.68 (d, J = 0.8 Hz, 1H). ^{13}C NMR (100 MHz, $CDCl_3$): δ 55.9, 56.0, 59.8, 60.7, 108.0, 111.1, 112.7, 118.9, 119.6, 127.7, 147.7, 149.3, 149.7, 151.2, 182.1. HRMS (ESI): calcd for $C_{15}H_{13}O_5$ [M − H] 273.0763, found 273.0766.

*[3-(3,4,5-Trimethoxyphenyl)oxiran-2-yl]phenylmethanone (**1f**).*[13] White solid. Yield: 5.85 g, 93%. Mp: 111−112 °C. ^{1}H NMR ($CDCl_3$, 400 MHz): δ3.87 (s, 3H), 3.89 (s, 6H), 4.04 (d, J = 1.6 Hz, 1H), 4.27 (d, J = 2.0 Hz, 1H), 6.60 (s, 2H), 7.51 (t, J = 7.6 Hz, 2H), 7.62−7.66 (m, 1H), 8.03 (d, J = 7.2 Hz, 2H).

*Phenyl(3-phenyloxiran-2-yl)methanone (**1g**).*[14] White solid. Yield: 4.04 g, 90%. Mp: 83−84 °C. ^{1}H NMR ($CDCl_3$, 400 MHz): δ 4.09 (s, 1H), 4.31 (d, J = 2.0 Hz, 1H), 7.37−7.43 (m, 5H), 7.50 (t, J = 7.6 Hz, 2H), 7.63 (t, J = 7.6 Hz, 1 H), 8.02 (d, J = 8.0 Hz, 2H).

*[3-(4-Methoxyphenyl)oxiran-2-yl]phenylmethanone (**1h**).*[15] White solid. Yield: 4.63 g, 91%. Mp: 77−78 °C. ^{1}H NMR ($CDCl_3$, 400 MHz): δ 3.83 (s, 3H), 4.03 (d, J = 2.0 Hz, 1H), 4.30 (d, J = 2.0 Hz, 1H), 6.94 (d, J = 8.8 Hz, 2H), 7.31 (d, J = 8.8 Hz, 2H), 7.50 (t, J = 7.6 Hz, 2H), 7.62 (t, J = 7.2 Hz, 1H), 8.02 (d, J = 7.2 Hz, 2H).

*[3-(4-Methoxyphenyl)oxiran-2-yl]-(4-methoxyphenyl)methanone (**1i**).*[16] White solid. Yield: 5.17 g, 91%. Mp: 116−117 °C. ^{1}H NMR ($CDCl_3$, 400 MHz): δ 3.83 (s, 3H), 3.98 (s, 3H), 4.02 (d, J = 2.0 Hz, 1H), 4.26 (d, J = 2.0 Hz, 1H), 6.93 (d, J = 8.8 Hz, 2H), 6.95 (d, J = 8.4 Hz, 2H), 7.30 (d, J = 8.8 Hz, 2H), 8.02 (d, J = 8.4 Hz, 2 H).

4.4. General Procedure for the Electrolysis of the Chalcone Epoxides. To an H-cell was added a solution of $LiClO_4$ supporting electrolyte (0.2 M) in CH_3CN and CH_2Cl_2 (50 mL, volume ratio = 4:1). Mediator, BMDPI, (0.1 mmol), chalcone epoxide **1** (1 mmol), and arylation reagent **2** (3 mmol) were added to the cell, respectively. At room temperature, the solution was electrolyzed at a controlled potential of 0.88 V vs $Ag/AgNO_3$ (0.1 M in CH_3CN) (the first oxidation peak of BMDPI). The working electrode was platinum net (25 mm × 35 mm) and the counter electrode was iron rod (d = 7 mm). The electrolysis was monitored by TLC and was terminated when the starting chalcone epoxide was consumed. After the electrolysis, the solvent of anode cell was removed by evaporation under reduced pressure. The residue was dissolved in 20 mL of dichloromethane and washed with 20 mL of water. The aqueous phase was extracted with dichloromethane (3 × 10 mL), the combined organic phases were dried by $MgSO_4$, and column chromatography on silica gel eluted with a mixture of petroleum ether and EtOAc gave the pure product.

*(2S,3S)-3-(3,4-Dimethoxyphenyl)-3-(furan-2-yl)-2-hydroxy-1-phenylpropan-1-one (**3a**).* Yellow oil. Yield: 105.7 mg, 30%. ^{1}H NMR ($CDCl_3$, 400 MHz): δ 3.70 (s, 3H), 3.76 (d, J = 6.8 Hz, 1H), 3.83 (s, 3H), 4.49 (d, J = 2.8 Hz, 1H), 5.84 (dd, J = 6.8, 2.8 Hz, 1H), 6.33−6.36 (m, 2H), 6.49−6.52 (m, 2H), 7.70 (d, J = 8.8 Hz, 1H), 7.38 (s, 1H), 7.54 (t, J = 7.6 Hz, 2H), 7.66 (t, J = 7.6 Hz, 1H), 7.90 (d, J = 7.2 Hz, 2H). ^{13}C NMR (100 MHz, $CDCl_3$): δ 49.2, 55.6, 55.7, 74.6, 107.8, 110.4, 110.7, 112.5, 121.5, 127.6, 128.6, 129.0, 134.0, 134.2, 141.6, 148.4, 148.5, 154.6, 199.9. HRMS (ESI) calcd for $C_{21}H_{20}NaO_5$ [M + Na] 375.1208, found 375.1208.

*(2S,3R)-3-(3,4-Dimethoxyphenyl)-3-(furan-2-yl)-2-hydroxy-1-phenylpropan-1-one (**4a**).* Yellow oil. Yield: 148.0 mg, 42%. ^{1}H NMR ($CDCl_3$, 400 MHz): δ3.86 (s, 3H), 3.87 (s, 3H), 3.87 (d, J = 6.8 Hz, 1H), 4.50 (d, J = 3.2 Hz, 1H), 5.53 (dd, J = 7.2, 3.2 Hz, 1H), 5.98 (d, J = 3.2 Hz, 1H), 6.25 (dd, J = 3.2, 1.6 Hz, 1H), 6.82 (d, J = 8.4 Hz, 1H), 6.98−7.03 (m, 2H), 7.29 (dd, J = 2.0, 0.8 Hz, 1H), 7.49 (t, J = 7.6 Hz, 2H), 7.62 (t, J = 7.6 Hz, 1H), 7.90 (d, J = 8.4 Hz, 2H). ^{13}C NMR (100 MHz, $CDCl_3$): δ 49.5, 55.9, 75.9, 108.6, 110.2, 111.1, 112.2, 120.9, 128.5, 128.9, 131.5, 133.8, 134.4, 141.8, 148.4, 148.9, 152.7, 200.6. HRMS (ESI): calcd for $C_{21}H_{20}NaO_5$ [M + Na] 375.1208, found 375.1197.

*(2S,3R)-3-(3,4-Dimethoxyphenyl)-2-hydroxy-3-(1-methyl-1H-pyrrol-2-yl)-1-phenylpropan-1-one (**3b**).* Obtained using the general electrolysis procedure as a yellow oil. Yield: 98.7 mg, 27%. ^{1}H NMR ($CDCl_3$, 400 MHz): δ 3.13 (s, 3H), 3.46 (d, J = 8.0 Hz, 1H), 3.69 (s, 3H), 3.82 (s, 3H), 4.39 (s, 1H), 5.82 (dd, J = 7.6, 2.0 Hz, 1H), 6.17 (t, J = 3.2 Hz, 1H), 6.35 (dd, J = 4.0, 2.4 Hz, 2H), 6.54 (d, J = 2.0 Hz, 1H), 6.65−6.69 (m, 2H), 7.55 (t, J = 7.6 Hz, 2H), 7.68 (t, J = 7.6 Hz, 1H), 7.96 (d, J = 7.6 Hz, 2H). ^{13}C NMR (100 MHz, $CDCl_3$): δ 34.1, 47.2, 55.7, 75.2, 106.6, 108.2, 110.6, 112.5, 121.5, 122.0, 128.7, 129.2, 132.5, 134.1, 148.1, 148.5, 200.0. HRMS (ESI): calcd for $C_{22}H_{24}NO_4$ [M + H] 366.1705, found 366.1700.

*(2S,3S)-3-(3,4-Dimethoxyphenyl)-2-hydroxy-3-(1-methyl-1H-pyrrol-2-yl)-1-phenylpropan-1-one (**4b**).* General electrolysis procedure. Yellow oil. Yield: 179.1 mg, 49%. ^{1}H NMR ($CDCl_3$, 400 MHz): δ 3.08 (s, 3H), 3.75 (d, J = 6.4 Hz, 1H), 3.78 (s, 3H), 3.80 (s, 3H), 4.44 (d, J = 5.2 Hz, 1H), 5.56 (t, J = 6.0 Hz, 1H), 6.08−6.09 (m, 1H), 6.24−6.25 (m, 1H), 6.45 (s, 1H), 6.70−6.80 (m, 3H), 7.42 (t, J = 7.6 Hz, 2H), 7.55 (t, J = 7.6 Hz, 1H), 7.74 (d, J = 7.2 Hz, 2H). ^{13}C NMR (100 MHz, $CDCl_3$): δ 33.8, 47.6, 55.8, 55.9, 76.0, 106.8, 108.3, 111.2, 112.0, 120.7, 122.1, 128.3, 128.6, 129.3, 132.0, 133.5, 135.0, 148.0, 148.9, 201.2. HRMS (ESI): calcd for $C_{22}H_{24}NO_4$ [M + H] 366.1705, found 366.1694.

*(2S,3R)-3-(3,4-Dimethoxyphenyl)-2-hydroxy-1-phenyl-3-(1H-pyrrol-2-yl)propan-1-one (**3c**).* Brown solid. Yield: 56.2 mg, 16%. Mp: 52−53 °C. ^{1}H NMR ($CDCl_3$, 400 MHz): δ 3.65 (s, 3H), 3.80 (s, 3H), 3.98 (d, J = 7.2 Hz, 1H), 4.58 (s, 1H), 5.73 (dd, J = 7.2, 2.0 Hz, 1H), 6.12 (s, 1H), 6.20 (dd, J = 5.6, 3.2 Hz, 1H), 6.32 (d, J = 1.6 Hz, 1H), 6.40 (dd, J = 8.4, 2.0 Hz, 1H), 6.65 (d, J = 8.4 Hz, 1H), 6.79−6.80 (m, 1H), 7.56 (t, J = 7.6 Hz, 2H), 7.69 (t, J = 7.6 Hz, 1H), 7.93 (d, J = 6.8 Hz, 2H), 9.17 (bs, 1H). ^{13}C NMR (100 MHz, $CDCl_3$): δ 47.9, 55.6, 55.7, 76.2, 106.4, 108.1, 110.7, 112.0, 117.3, 121.0, 128.2, 129.2 130.0, 132.0, 134.0, 134.3, 148.1, 148.3, 199.6. HRMS (ESI): calcd for $C_{21}H_{22}NO_4$ [M + H] 352.1549, found 352.1552; calcd for $C_{21}H_{20}NO_4$ [M − H] 350.1392, found 350.1406.

*(2S,3S)-3-(3,4-Dimethoxyphenyl)-2-hydroxy-1-phenyl-3-(1H-pyrrol-2-yl)propan-1-one (**4c**).* General electrolysis procedure. Purple solid. Yield: 80.8 mg, 23%. Mp: 92−94 °C. ^{1}H NMR ($CDCl_3$, 400 MHz): δ 3.83 (s, 3H), 3.86 (s, 3H), 3.95 (d, J = 5.6 Hz, 1H), 4.51 (d, J = 2.8 Hz, 1H), 5.65−5.68 (m, 2H), 6.05 (dd, J = 5.6, 2.8 Hz, 1H), 6.67−6.68 (m, 1H), 6.82 (d, J = 8.0 Hz, 1H), 6.92−6.93 (m, 1H), 7.03 (dd, J = 8.4, 2.0 Hz, 1H), 7.49 (t, J = 7.6 Hz, 2H), 7.62 (t, J = 7.6 Hz, 1H), 7.84 (d, J = 7.2 Hz, 2H), 8.39 (bs, 1H). ^{13}C NMR (100 MHz, $CDCl_3$): δ 48.0, 55.9, 76.3, 107.5, 107.6, 111.2, 111.8, 117.9, 120.4, 128.5, 128.5, 128.9, 133.0, 133.9, 134.2, 148.0, 149.0, 200.8. HRMS (ESI) calcd for $C_{21}H_{22}NO_4$ [M + H] 352.1549, foun: 352.1542; calcd for $C_{21}H_{20}NO_4$ [M − H] 350.1392, found 350.1407.

*(2S,3R)-3-(3,4-Dimethoxyphenyl)-2-hydroxy-3-(1-methyl-1H-indol-3-yl)-1-phenylpropan-1-one (**3d**).* Yellow solid. Yield: 216.1 mg, 52%. Mp: 71−72 °C. ^{1}H NMR ($CDCl_3$, 400 MHz): δ 3.66 (s, 3H), 3.76−3.82 (m, 7H), 4.74 (s, 1H), 5.83 (d, J = 5.2 Hz, 1H), 6.52 (s, 1H), 6.56 (d, J = 8.4 Hz, 1H), 6.64 (d, J = 8.4 Hz, 1H), 6.94 (t, J = 7.2 Hz, 1H), 7.17 (t, J = 8.0 Hz, 2H), 7.29 (d, J = 8.0 Hz, 1H), 7.50−7.53 (m, 3H), 7.65 (t, J = 7.6 Hz, 1H) 7.92 (d, J = 7.6 Hz, 2H). ^{13}C NMR (100 MHz, $CDCl_3$): δ 32.8, 46.8, 55.7, 76.3, 109.2, 110.6, 112.6, 115.4, 118.9, 119.2, 121.4, 121.7, 127.4, 127.7, 128.6, 129.1, 130.5, 134.0, 134.4, 136.9, 148.0, 148.3, 200.5. HRMS (ESI) calcd for $C_{26}H_{26}NO_4$ [M + H] 416.1862, found 416.1852.

*(2S,3S)-3-(3,4-Dimethoxyphenyl)-2-hydroxy-3-(1-methyl-1H-indol-3-yl)-1-phenylpropan-1-one (**4d**).* Yellow solid. Yield: 128.8 mg, 31%. Mp: 69−70 °C. ^{1}H NMR ($CDCl_3$, 400 MHz): δ 3.72 (s, 3H), 3.77−3.88 (m, 7H), 4.82 (d, J = 2.4 Hz, 1H), 5.76 (dd, J = 7.2, 2.8 Hz, 1H), 6.80−6.86 (m, 2H), 6.92 (d, J = 8.0 Hz, 1H), 6.95 (s, 1H), 7.06−7.12 (m, 3H), 7.21 (d, J = 8.0 Hz, 1H), 7.48 (t, J = 8.0 Hz, 2H), 7.63 (t, J = 7.2 Hz, 1H), 7.83 (d, J = 7.6 Hz, 2H). ^{13}C NMR (100 MHz, $CDCl_3$): δ 32.8, 46.2, 55.9, 56.0, 76.4, 77.3, 109.1, 111.1, 111.3, 112.0, 118.7, 119.0, 120.3, 121.4, 127.7, 128.4, 128.7, 128.8, 133.8, 134.4, 135.5, 136.5, 147.8, 148.9, 200.9. HRMS (ESI): calcd for $C_{26}H_{24}NO_4$ [M − H] 414.1705, found 414.1708.

*(2S,3R)-3-(3,4-Dimethoxyphenyl)-2-hydroxy-3-(1H-indol-3-yl)-1-phenylpropan-1-one (**3e**).* Yellow solid. Yield: 164.6 mg, 41%. Mp:

dx.doi.org/10.1021/jo5022184 | J. Org. Chem. 2015, 80, 781−789

169−170 °C. ^{1}H NMR ($CDCl_3$, 400 MHz): δ 3.64 (s, 3H), 3.78−3.79 (m, 4H), 4.74 (s, 1H), 5.85 (s, 1H), 6.49−6.52 (m, 2H), 6.64 (d, J = 8.0 Hz, 1H), 6.93 (t, J = 7.6 Hz, 1H), 7.11−7.19 (m, 2H), 7.33 (d, J = 8.0 Hz, 1H), 7.52 (t, J = 7.6 Hz, 2H), 7.64−7.66 (m, 2H), 7.93 (d, J = 7.6 Hz, 2H), 8.26 (bs, 1H). ^{13}C NMR (100 MHz, $CDCl_3$): δ 46.8, 55.6, 55.7, 76.2, 110.6, 111.2, 112.6, 116.9, 119.1, 119.4, 121.5, 122.1, 123.0, 127.0, 128.7, 129.1, 130.3, 134.0, 134.4, 136.1, 148.0, 148.2, 200.5. HRMS (ESI) calcd for $C_{25}H_{22}NO_4$ [M − H] 400.1549, found 400.1556.

*(2S,3S)-3-(3,4-Dimethoxyphenyl)-2-hydroxy-3-(1H-indol-3-yl)-1-phenylpropan-1-one (**4e**).* Yellow solid. Yield: 164.6 mg, 41%. Mp: 85−86 °C. ^{1}H NMR ($CDCl_3$, 400 MHz): δ 3.82 (s, 3H), 3.86 (s, 3H), 3.90 (d, J = 5.2 Hz, 1H), 4.84 (d, J = 2.8 Hz, 1H), 5.79 (bs, 1H), 6.81−6.88 (m, 2H), 6.97 (d, J = 8.0 Hz, 1H), 7.04−7.12 (m, 4H), 7.29 (d, J = 8.0 Hz, 1H), 7.49 (t, J = 7.6 Hz, 2H), 7.73 (t, J = 7.6 Hz, 1H), 7.84 (d, J = 7.2 Hz, 2H), 8.07 (bs, 1H). ^{13}C NMR (100 MHz, $CDCl_3$): δ 46.2, 55.9, 55.9, 76.5, 111.0, 111.1, 112.0, 112.9, 119.1, 119.2, 120.4, 121.9, 123.6, 127.2, 128.6, 128.8, 133.8, 134.4, 135.1, 135.7, 147.8, 148.8, 201.0. HRMS (ESI) calcd for $C_{25}H_{24}NO_4$ [M + H] 402.1705, found 402.1705.

*(2S,3S)-3-(3,4-Dimethoxyphenyl)-3-(furan-2-yl)-2-hydroxy-1-(4-methoxypheny)propan-1-one (**3f**).* White solid. Yield: 61.2 mg, 16%. Mp: 118−119 °C. ^{1}H NMR ($CDCl_3$, 400 MHz): δ 3.71 (s, 3H), 3.83 (s, 3H), 3.90 (s, 3H), 4.48 (d, J = 2.0 Hz, 1H), 5.78 (s, 1H), 6.35 (s, 2H), 6.52 (d, J = 8.0 Hz, 1H), 6.56 (s, 2H), 6.70 (d, J = 8.0 Hz, 1H), 7.00 (d, J = 8.4 Hz, 2H), 7.37 (s, 1H), 7.90 (d, J = 8.4 Hz, 2H). ^{13}C NMR (100 MHz, $CDCl_3$): δ 49.6, 55.6, 55.7, 74.2, 107.7, 110.4, 110.6, 112.6, 114.3, 121.5, 126.8, 127.8, 130.9, 141.6, 148.4, 148.4, 154.8, 164.2, 198.0. HRMS (ESI): calcd for $C_{22}H_{23}O_6$ [M + H] 383.1495, found 383.1480; calcd for $C_{22}H_{22}NaO_6$ [M + Na] 405.1314, found 405.1297.

*(2S,3R)-3-(3,4-Dimethoxyphenyl)-3-(furan-2-yl)-2-hydroxy-1-(4-methoxypheny)propan-1-one (**4f**).* White solid. Yield: 61.2 mg, 16%. Mp: 102−103 °C. ^{1}H NMR ($CDCl_3$, 400 MHz): δ 3.87−3.93 (m, 10H), 4.50 (d, J = 3.2 Hz, 1H), 5.50 (bs, 1H), 6.02 (d, J = 3.2 Hz, 1H), 6.25 (dd, J = 3.2, 2.0 Hz, 1H), 6.82 (d, J = 8.0 Hz, 1H), 6.96 (d, J = 8.8 Hz, 2H), 7.01 (dd, J = 8.4, 1.6 Hz, 1H), 7.04 (d, J = 1.6 Hz, 1H), 7.30 (d, J = 0.8 Hz, 1H), 7.86 (d, J = 8.0 Hz, 2H). ^{13}C NMR (100 MHz, $CDCl_3$): δ 49.8, 55.6, 55.9, 75.4, 108.5, 110.2, 111.1, 112.2, 114.1, 120.9, 127.0, 130.9, 131.7, 141.8, 148.3, 148.9, 152.8, 164.1, 198.6. HRMS (ESI): calcd for $C_{22}H_{22}NaO_6$ [M + Na] 405.1314, found 405.1316.

*(2S,3S)-1-(4-Chlorophenyl)-3-(3,4-dimethoxyphenyl)-3-(furan-2-yl)-2-hydroxypropan-1-one (**3g**).* Yellow solid. Yield: 108.3 mg, 28%. Mp: 103−104 °C. ^{1}H NMR ($CDCl_3$, 400 MHz): δ 3.68 (d, J = 7.2 Hz, 1H), 3.73 (s, 3H), 3.83 (s, 3H), 4.43 (d, J = 2.8 Hz, 1H), 5.78 (dd, J = 7.2 Hz, 3.2 Hz, 1H), 6.30 (d, J = 3.2 Hz 1H), 6.35 (d, J = 3.2 Hz, 1H), 6.50 (dd, J = 8.0, 1.6 Hz, 1H), 6.58 (d, J = 2.0 Hz, 1H), 6.70 (d, J = 8.4 Hz, 1H), 7.37 (s, 1H), 7.51 (d, J = 8.4 Hz, 2H), 7.83 (d, J = 8.4 Hz, 2H). ^{13}C NMR (100 MHz, $CDCl_3$): δ 49.3, 55.8, 55.8, 74.7, 107.9, 110.4, 110.8, 112.4, 121.5, 127.6, 129.4, 129.9, 132.5, 132.5, 140.5, 141.7, 148.6, 154.2, 198.8. HRMS (ESI): calcd for $C_{21}H_{18}ClO_5$ [M − H] 385.0843, found 385.0858.

*(2S,3R)-1-(4-Chlorophenyl)-3-(3,4-dimethoxyphenyl)-3-(furan-2-yl)-2-hydroxypropan-1-one (**4g**).* Yellow solid. Yield: 150.9 mg, 39%. Mp: 107−108 °C. ^{1}H NMR ($CDCl_3$, 400 MHz): δ 3.77 (d, J = 7.2 Hz, 1H), 3.83(s, 3H), 3.86 (s, 3H), 4.45 (d, J = 3.6 Hz, 1H), 5.48 (dd, J = 7.2, 4.0 Hz, 1H), 6.00 (d, J = 2.8 Hz, 1H), 6.25 (dd, J = 3.2, 2.0 Hz, 1H), 6.80 (d, J = 8.4 Hz, 1H), 6.96 (dd, J = 8.0, 1.6 Hz, 1H), 7.00 (d, J = 2.0 Hz, 1H), 7.30 (s, 1H), 7.45 (d, J = 8.4 Hz, 2H), 7.78 (d, J = 8.8 Hz, 2H). ^{13}C NMR (100 MHz, $CDCl_3$): δ 49.6, 55.9, 75.9, 108.7, 110.3, 111.2, 112.2, 120.9, 129.2, 129.8, 131.1, 132.8, 140.2, 141.9, 148.5, 149.0, 152.6, 199.5. HRMS (ESI): calcd for $C_{21}H_{18}ClO_5$ [M − H] 385.0843, found 385.0861.

*(2S,3S)-1-(3-Chlorophenyl)-3-(3,4-dimethoxyphenyl)-3-(furan-2-yl)-2-hydroxypropan-1-one (**3h**).* General electrolysis procedure. Yellow oil. Yield: 100.6 mg, 26%. ^{1}H NMR ($CDCl_3$, 400 MHz): δ 3.66 (d, J = 7.2 Hz, 1H), 3.45 (s, 3H), 3.85 (s, 3H), 4.45 (d, J = 2.8 Hz, 1H), 5.79 (dd, J = 7.2, 3.2 Hz, 1H), 6.31 (d, J = 3.2 Hz, 1H), 6.34 (dd, J = 2.8, 2.0 Hz, 1H), 6.55−6.57 (m, 2H), 6.73 (d, J = 8.0 Hz, 1H), 7.38 (d, J = 1.6 Hz, 1H), 7.48 (t, J = 8.0 Hz, 1H), 7.62−7.64 (m, 1H), 7.78 (d, J = 7.6 Hz, 1H), 7.83 (s, 1H). ^{13}C NMR (100 MHz, $CDCl_3$): δ 49.2, 55.7, 55.8, 74.8, 108.0, 110.5, 110.8, 112.3, 121.4, 126.6, 127.6, 128.5, 130.3, 133.9, 135.4, 135.8, 141.8, 148.5, 148.6, 154.1, 199.0. HRMS (ESI): calcd for $C_{21}H_{18}ClO_5$ [M − H] 385.0843, found 385.0854.

*(2S,3R)-1-(3-Chlorophenyl)-3-(3,4-dimethoxyphenyl)-3-(furan-2-yl)-2-hydroxypropan-1-one (**4h**).* Yellow oil. Yield: 181.8 mg, 47% ^{1}H NMR ($CDCl_3$, 400 MHz): δ 3.70 (d, J = 7.6 Hz, 1H), 3.85(s, 3H), 3.86 (s, 3H), 4.44 (d, J = 4.0 Hz, 1H), 5.48 (dd, J = 7.2, 4.0 Hz, 1H), 6.03 (d, J = 3.2 Hz, 1H), 6.27 (dd, J = 3.2, 1.6 Hz, 1H), 6.81 (d, J = 8.8 Hz, 1H), 6.95−6.97 (m, 2H), 7.32 (s, 1H), 7.41 (t, J = 8.0 Hz, 1H), 7.55−7.58 (m, 1H), 7.70 (d, J = 8.0 Hz, 1H), 7.79 (t, J = 1.6 Hz, 1H). ^{13}C NMR (100 MHz, $CDCl_3$): δ 49.7, 55.9, 76.0, 108.7, 110.3, 111.1, 112.1, 120.9, 126.4, 128.6, 130.1, 130.9, 133.6, 135.1, 136.2, 141.9, 148.4, 148.9, 152.6, 199.7. HRMS (ESI): calcd for $C_{21}H_{18}ClO_5$ [M − H] 385.0843, found 385.0843.

*(2S,3S)-3-(3,4-Dimethoxyphenyl)-1,3-di(furan-2-yl)-2-hydroxypropan-1-one (**3i**).* Yellow solid. Yield: 82.2 mg, 24%. Mp: 54−55 °C. ^{1}H NMR ($CDCl_3$, 400 MHz): δ 3.54 (d, J = 7.2 Hz, 1H), 3.75(s, 3H), 3.83 (s, 3H), 4.66 (d, J = 3.2 Hz, 1H), 5.48 (dd, J = 7.2, 3.2 Hz, 1H), 6.32−6.35 (m, 2H), 6.59−6.66 (m, 3H), 6.72 (d, J = 8.0 Hz, 1H), 7.32 (d, J = 3.6 Hz, 1H), 7.38 (s, 1H), 7.70 (d, J = 0.8 Hz, 1H). ^{13}C NMR (100 MHz, $CDCl_3$): δ 49.0, 55.7, 75.1, 107.8, 110.4, 110.7, 112.3, 112.8, 119.2, 121.4, 128.1, 141.6, 147.3, 148.4, 148.5, 150.5, 154.8, 188.0. HRMS (ESI): calcd for $C_{19}H_{18}NaO_6$ [M + Na] 365.1001, found 365.0999.

*(2S,3R)-3-(3,4-Dimethoxyphenyl)-1,3-di(furan-2-yl)-2-hydroxypropan-1-one (**4i**).* White solid. Yield: 130.1 mg, 38%. Mp: 118−119 °C. ^{1}H NMR ($CDCl_3$, 400 MHz): δ 3.60 (d, J = 7.6 Hz, 1H), 3.88(s, 3H), 3.89 (s, 3H), 4.66 (d, J = 4.4 Hz, 1H), 5.28 (dd, J = 7.6, 4.0 Hz, 1H), 6.10 (d, J = 3.2 Hz, 1H), 6.28 (dd, J = 2.8, 1.6 Hz, 1H), 6.57 (dd, J = 3.6, 1.6 Hz, 1H), 6.82 (d, J = 8.4 Hz, 1H), 6.98−7.01 (m, 2H), 7.25−7.26 (m, 1H), 7.32 (s, 1H), 7.63 (s, 1H). ^{13}C NMR (100 MHz, $CDCl_3$): δ 49.3, 55.9, 76.2, 108.5, 110.3, 111.1, 112.1, 112.7, 119.2, 120.9, 131.3, 141.9, 147.2, 148.3, 148.9, 150,7, 152.8, 188.4. HRMS (ESI): calcd for $C_{19}H_{18}NaO_6$ [M + Na] 365.1001, found 365.0995.

*(2S,3S)-3-(Furan-2-yl)-2-hydroxy-1-phenyl-3-(3,4,5-trimethoxyphenyl)propan-1-one (**3j**).*[8] White solid. Yield: 99.4 mg, 26%. Mp: 102−103 °C. ^{1}H NMR ($CDCl_3$, 400 MHz): δ 3.66 (s, 6H), 3.77−3.81 (m, 4H), 4.48 (s, 1H), 5.82 (d, J = 4.4 Hz, 1H), 6.16 (s, 2H), 6.37 (s, 1H), 6.40 (s, 1H), 7.38 (s, 1H), 7.54 (t, J = 7.2 Hz, 2H), 7.67 (t, J = 7.2 Hz, 1H), 7.89 (d, J = 7.6 Hz, 2 H). HRMS (ESI): calcd for $C_{22}H_{22}NaO_6$ [M + Na] 405.1314, found: 405.1314.

*(2S,3R)-3-(Furan-2-yl)-2-hydroxy-1-phenyl-3-(3,4,5-trimethoxyphenyl)propan-1-one (**4j**).*[8] White solid. Yield: 130.0 mg, 34%. Mp: 99−100 °C. ^{1}H NMR ($CDCl_3$, 400 MHz): δ 3.77−3.87 (m, 10H), 4.44 (s, 1H), 5.55 (d, J = 4.4 Hz, 1H), 6.05 (s, 1H), 6.27 (s, 1H), 6.40 (s, 2H), 7.38 (s, 1H), 7.48 (t, J = 6.8 Hz, 2H), 7.60 (t, J = 6.8 Hz, 1H), 7.83 (d, J = 7.2 Hz, 2 H). HRMS (ESI): calcd for $C_{22}H_{22}NaO_6$ [M + Na] 405.1314, found 405.1303.

■ ASSOCIATED CONTENT

Supporting Information

Full experimental details, characterization data, copies of ^{1}H and ^{13}C NMR spectra for all compounds, and HRMS spectra for new compounds. This material is available free of charge via the Internet at http://pubs.acs.org/.

■ AUTHOR INFORMATION

Corresponding Authors

*Tel: 0086-10-67396211. Fax: 0086-10-67396211. E-mail: zengcc@bjut.edu.cn.

*E-mail: little@chem.ucsb.edu.

Notes

The authors declare no competing financial interest.

■ ACKNOWLEDGMENTS

This work was supported by grants from the National Natural Science Foundation of China (Nos. 21272021 and 21472011), the National Key Technology R&D Program (2011BAD23B01), and funding to C.-C.Z. from the Beijing City Education Committee (KM201010005009). C.-C.Z. and R.D.L. are grateful to the US National Science Foundation supported PIRE-ECCI Program (OISE-0968399) for fostering our international collaboration.

■ REFERENCES

(1) For some excellent reviews on organic electrochemical reactions for synthesis, see: (a) Yoshida, J.; Kataoka, K.; Horcajada, R.; Nagaki, A. *Chem. Rev.* **2008**, *108*, 2265. (b) Sperry, J. B.; Wright, D. L. *Chem. Soc. Rev.* **2006**, *35*, 605. (c) Moeller, K. D. *Tetrahedron* **2000**, *56*, 9527. (d) Lund, H. *J. Electrochem. Soc.* **2002**, *149*, S21.

(2) For recent examples on direct electrolysis, see: (a) Elsler, B.; Schollmeyer, D.; Dyballa, K. M.; Franke, R.; Waldvogel, S. R. *Angew. Chem., Int. Ed.* **2014**, *53*, 5210. (b) Morofuji, T.; Shimizu, A.; Yoshida, J.-i. *J. Am. Chem. Soc.* **2014**, *136*, 4496. (c) Morofuji, T.; Shimizu, A.; Yoshida, J. *J. Am. Chem. Soc.* **2013**, *135*, 5000. (d) Kakiuchi, F.; Kochi, T.; Mutsutani, H.; Kobayashi, N.; Urano, S.; Sato, M.; Nishiyama, S.; Tanabe, T. *J. Am. Chem. Soc.* **2009**, *131*, 11310. (e) Kirste, A.; Schnakenburg, G.; Stecker, F.; Fischer, A.; Waldvogel, S. R. *Angew. Chem., Int. Ed.* **2010**, *49*, 971. (f) Kirste, A.; Elsler, B.; Schnakenburg, G.; Waldvogel, S. R. *J. Am. Chem. Soc.* **2012**, *134*, 3571. (g) Morofuji, T.; Shimizu, A.; Yoshida, J. *Angew. Chem., Int. Ed.* **2012**, *51*, 7259.

(3) For reviews on indirect electrolysis, see: (a) Francke, R.; Little, R. D. *Chem. Soc. Rev.* **2014**, *43*, 2492. (b) Ogibin, Y. N.; Elinson, M. N.; Nikishin, G. I. *Russ. Chem. Rev.* **2009**, *78*, 89. (c) Steckhan, E. *Angew. Chem., Int. Ed. Engl.* **1986**, *25*, 683. For recent examples on indirect electrolysis, see: (d) Kajiyama, D.; Saitoh, T.; Nishiyama, S. *Electrochemistry* **2013**, *81*, 319. (e) Gao, X.-F.; Yuan, G.-Q.; Chen, H.-J.; Jiang, H.-F.; Li, Y.-W.; Qi, C.-R. *Electrochem. Commun.* **2013**, *34*, 242. (f) Li, W.-C.; Zeng, C.-C.; Hu, L.-M.; Tian, H.-Y.; Little, R. D. *Adv. Synth. Catal.* **2013**, *355*, 2884. (g) Zhang, Z.-L.; Su, J.-H.; Zha, Z.-G.; Wang, Z.-Y. *Chem.—Eur. J.* **2013**, *19*, 17711.

(4) Zhang, N. T.; Zeng, C. C.; Lam, C. M.; Gbur, R. K.; Little, R. D. *J. Org. Chem.* **2013**, *78*, 2104.

(5) Francke, R.; Little, R. D. *J. Am. Chem. Soc.* **2014**, *136*, 427.

(6) Lu, N. N.; Yoo, S. J.; Li, L. J.; Zeng, C. C.; Little, R. D. *Electrochim. Acta* **2014**, *142*, 254.

(7) Zeng, C.-C.; Zhang, N.-T.; Lam, C. M.; Little, R. D. *Org. Lett.* **2012**, *14*, 1314.

(8) Hou, C.-D.; Cu, X.-L.; Jia, X.-D.; Wang, X.-C.; An, J.-Z.; Sun, C.-G. *Tetrahedron* **2012**, *68*, 190.

(9) A classical current−time curve for an indirect electrolysis consists of initial decrease of current intensity, followed by a plateau curve and another sharp drop of current intensity. Although we have noticed a slight increase of current intensity before it drops sharply in Figure 3, we believe that Figure 3 primarily follows the classical behavior of current−time curve. We postulate that the irregularity may come from the disturbance of the solution due to the stirring of the solution and/or the changes of electrode surface during the removal/reinsertion of the working electrode for TLC analysis.

(10) (a) Halas, S. M.; Okyne, K.; Fry, A. J. *Electrochim. Acta* **2003**, *48*, 1837. (b) Purgato, F. L. S.; Ferreira, M. I. C.; Romero, J. R. *J. Mol. Catal. A: Chem.* **2000**, *161*, 99.

(11) Eneback, C. *Acta Chem. Scand.* **1958**, *12*, 1528.

(12) Bhat, B. A.; Dhar, K. L.; Puri, S. C.; Saxena, A. K.; Shanmugavel, M.; Qazi, G. N. *Bioorg. Med. Chem. Lett.* **2005**, *15*, 3177.

(13) Hou, C.-D.; An, J.; Xu, X.; Jia, X.-D.; Wang, X.-C.; Kang, L. *Tetrahedron Lett.* **2013**, *54*, 1145.

(14) Geng, X.; Wang, Z.; Li, X.; Zhang, C. *J. Org. Chem.* **2005**, *70*, 9610.

(15) Kumar, C. V.; Ramaiah, D.; Das, P. K.; George, M. V. *J. Org. Chem.* **1985**, *50*, 2818.

(16) Li, J.; Yin, Y.; Sun, M. *Ultrason. Sonochem.* **2010**, *17*, 363.